

# RNA silencing of the mitochondrial ABCB7 transporter in HeLa cells causes an iron-deficient phenotype with mitochondrial iron overload

Patrizia Cavadini,<sup>1</sup> Giorgio Biasiotto,<sup>1</sup> Maura Poli,<sup>1</sup> Sonia Levi,<sup>2</sup> Rosanna Verardi,<sup>3</sup> Isabella Zanella,<sup>1</sup> Manuela Derosas,<sup>1</sup> Rosaria Ingrassia,<sup>1</sup> Marcella Corrado,<sup>1</sup> and Paolo Arosio<sup>1</sup>

<sup>1</sup>Dipartimento Materno Infantile e Tecnologie Biomediche, University of Brescia, Spedali Civili, Brescia, Italy; <sup>2</sup>Unit of Proteomics of Iron Metabolism, Vita e Salute San Raffaele University, Milan, Italy; <sup>3</sup>Section of Immunohematology and Transfusional Medicine, Spedali Civili, Brescia, Italy

**X-linked sideroblastic anemia with ataxia (XLSA/A) is caused by defects of the transporter ABCB7 and is characterized by mitochondrial iron deposition and excess of protoporphyrin in erythroid cells. We describe ABCB7 silencing in HeLa cells by performing sequential transfections with siRNAs. The phenotype of the ABCB7-deficient cells was characterized by a strong reduction in proliferation rate that was not rescued by iron supplementation, by evident signs of iron deficiency,**

**and by a large approximately 6-fold increase of iron accumulation in the mitochondria that was poorly available to mitochondrial ferritin. The cells showed an increase of protoporphyrin IX, a higher sensitivity to H<sub>2</sub>O<sub>2</sub> toxicity, and a reduced activity of mitochondrial superoxide dismutase 2 (SOD2), while the activity of mitochondrial enzymes, such as citrate synthase or succinate dehydrogenase, and ATP content were not decreased. In contrast, aconitase activity, particularly**

**that of the cytosolic, IRP1 form, was reduced. The results support the hypothesis that ABCB7 is involved in the transfer of iron from mitochondria to cytosol, and in the maturation of cytosolic Fe/S enzymes. In addition, the results indicate that anemia in XLSA/A is caused by the accumulation of iron in a form that is not readily usable for heme synthesis. (Blood. 2007;109:3552-3559)**

© 2007 by The American Society of Hematology

## Introduction

Iron is essential in all eukaryotes for various vital functions including respiration, gene regulation, and DNA replication and repair. However, iron is also potentially toxic and dysregulation of its homeostasis may contribute to various hematologic, metabolic, and neurodegenerative diseases.<sup>1</sup> Mitochondria play a central role in iron metabolism, since the mitochondrion is the place of synthesis of heme and iron sulfur (Fe/S) proteins,<sup>2</sup> and dysregulation of mitochondrial iron is associated with certain diseases.<sup>3</sup> Among them is Friedreich ataxia, which is caused by deficiency of frataxin, a protein involved in mitochondrial iron trafficking<sup>4</sup>; the X-linked sideroblastic anemia (XLSA) associated with deficiency of the erythroid-specific ALAS2<sup>5</sup>; and XLSA/A, X-linked sideroblastic anemia with ataxia associated with defects of the ABC transporter ABCB7.<sup>6</sup> Most of our understanding of mitochondrial iron trafficking comes from the extensive studies done on *S cerevisiae* that showed that the organelle is the only site for the synthesis of Fe/S clusters, and that this activity is essential for the cell.<sup>2,7</sup> This biochemical pathway necessitates more than 10 different components, which include the cysteine desulphurase Nfs1p; the scaffold proteins Isu1p/Isu2p; chaperones; and the redox enzymes Arh1p, Yah1p, and glutaredoxin-5.<sup>2</sup> The functionality of Fe/S biosynthesis is essential also for the assembly of extramitochondrial Fe/S enzymes, including Leu1p and Rli1p, the latter involved in ribosome biogenesis<sup>8,9</sup>; but biosynthesis requires a set of accessory proteins that include the ABC transporter named Atm1p, the sulphhydryl oxidase Erv1p of mitochondrial intermembrane space, glutathione, the cytosolic P-loop NTPase Cfd1p/Nbp35p, and the cytosolic iron-only hydrogenase-like Nar1p.<sup>10</sup>

The centrality of mitochondria in cellular iron homeostasis is also indicated by the evidence that yeast iron-regulon depends on Fe/S biogenesis.<sup>11,12</sup> The inactivation of any of the proteins for mitochondrial Fe/S biosynthesis causes a massive mitochondrial iron deposition, up to 30-fold above the normal; the alteration or inhibition of mitochondrial Fe/S enzymes such as aconitase and succinate dehydrogenase (SDH); the lack of growth on nonfermentable media; and signs of oxidative damage.<sup>13</sup> In contrast, the inactivation of the proteins for Fe/S export, such as Atm1p, causes mitochondrial iron accumulation without major effects on mitochondrial enzymes.<sup>7</sup> Most of these proteins have homologs in mammalian cells, but relatively little work has been dedicated to the study of Fe/S biogenesis in these cells, with the exception of frataxin.<sup>14</sup> Recently, it was shown that some key enzymes of Fe/S pathway, the cysteine desulphurase ISCS, and the scaffold proteins ISCU and NFSU show alternative splicing that produces cytosolic as well as mitochondrial proteins.<sup>15-17</sup> The cytosolic forms have been isolated and found to be functional, and it was demonstrated that cytosolic ISCU proteins participate in the synthesis of cytosolic Fe/S proteins such as the IRP1/c-aconitase.<sup>15,16</sup> However, other reports showed that the depletion of mitochondrial Nfs1 inhibited the formation of cytosolic Fe/S proteins in mammalian cells,<sup>18,19</sup> and the defect was not rescued by the expression of a cytosolic form of the cysteine desulphurase.<sup>18</sup>

ABCB7 is the human ortholog of Atm1p, and its expression in yeasts rescued the defects of Atm1p deficiency.<sup>20</sup> Three different mutations of ABCB7 are associated with sideroblastic anemia with ataxia and hypoplasia of the cerebellum (XLSA/A, OMIM 301310).

Submitted August 15, 2006; accepted November 22, 2006. Prepublished online as *Blood* First Edition Paper, December 27, 2006; DOI 10.1182/blood-2006-08-041632.

The publication costs of this article were defrayed in part by page charge

payment. Therefore, and solely to indicate this fact, this article is hereby marked "advertisement" in accordance with 18 USC section 1734.

© 2007 by The American Society of Hematology

They consist of missense mutations (I400M, E433K, and V411L) at the border of putative transmembrane domains of the protein and were found to rescue only partially the defects of Atm1p-deficient yeasts.<sup>6</sup> A study on erythroid cells showed that ABCB7 expression increases the activity of ferrochelatase by binding to its C-terminus.<sup>21</sup> The recent study of mice deficient in ABCB7 showed that the protein is essential in early gestation. The systemic and tissue-specific deletion of ABCB7 in most organs, including CNS and bone marrow, was lethal, with the notable exception of liver and endothelial cells.<sup>22</sup> Liver-specific ABCB7 deletion caused periportal hepatocellular iron deposition with characteristic round structures, the origin of which was unclear; a strong up-regulation of TfR1 expression, consistent with the activation of IRP1; and a paradoxical minor increase of ferritin.<sup>22</sup> Surprisingly, mitochondrial iron overload was not observed, and the activity of mitochondrial enzymes with Fe/S complexes such as ferrochelatase, m-aconitase, and succinate dehydrogenase was only marginally affected, while that of cytosolic enzymes such as c-aconitase or xanthine oxidase was strongly reduced.<sup>22</sup> These results confirm that the transporter has a major role in cellular iron homeostasis but do not clarify why ABCB7 deficiency may cause sideroblastic anemia and movement disorders. We used a simpler approach to analyze the effects of ABCB7 deficiency in cultured HeLa cells. We describe the conditions to silence the protein by using siRNAs, and we found that ABCB7 inhibition caused a strong reduction in cell proliferation, and a cytosolic iron deprivation accompanied by a large iron deposition in the mitochondria that was not available to mitochondrial ferritin. Protoporphyrin accumulation and the reduced availability of the mitochondrial iron may partially explain the development of anemia.

## Materials and methods

### Production of siRNAs

To produce double-stranded siRNAs by *in vitro* transcription, we followed the procedure described in Donze and Picard.<sup>23</sup> Briefly, we produced desoxy-oligonucleotides in which 22 nucleotides (nts) of sense or antisense sequence were flanked at 3' by the TATAGTGAGTCGTATTA sequence, complementary to T7 promoter. The sense sequences were the following: ABCB7-871 (at 871 nt from start codon), GTGCCAGTTTGGTTGGTAAC; ABCB7-792 (at 792 nt from start codon), CTGAGTGCTTTGGTATTTAATC; and ABCB7-1663 (at 1663 nt from start codon), ATGCTGTCTCTTCCATAATAC. All the sequences terminated with G and C, necessary for T7 polymerase activity. The oligonucleotides were annealed with the primer for T7 polymerase, and the enzyme was added. The 2 complementary transcripts were annealed, analyzed on polyacrylamide electrophoresis, and used for transfection. In most experiments, we used synthetic double-strand ABCB7-792 siRNA, which, like scrambled siRNA, was produced by Qiagen-Xeragon (Germantown, MD).

### HeLa cell transfection

HeLa cells were grown in RPMI medium (Life Technologies, Invitrogen, Bethesda, MD), 10% fetal bovine serum (Clontech, Palo Alto, CA), 100 U/mL penicillin, 100 mg/mL streptomycin, and 1 mM L-glutamine. With *in vitro*-transcribed siRNAs, 10<sup>5</sup> cells/well were seeded in the 12-well plates, transfected the following day with 100 pmol ds-siRNAs using Oligofectamine (Invitrogen, Paisley, United Kingdom) following the manufacturer's instructions, grown for 72 hours, and then harvested and analyzed. With a synthetic siRNA (ABCB7-792), the HeLa cells were subjected to 2 rounds of transfection at day 1 and day 4 and harvested at day 7. To verify transfection efficiency, HeLa cells were transfected under the same conditions with control, nonsilencing ds-siRNA labeled with rhodamine

(Qiagen-Xeragon), and inspection under the fluorescence microscope showed that more than 90% of the cells were labeled.

### Analysis of cell viability

To evaluate cell viability, the HeLa cells at day 7 after transfection were counted and the cells were grown for 3 days. Then all the cells were counted and evaluated for trypan blue exclusion. Alternatively, at day 6 after transfection, 2 × 10<sup>4</sup> cells were seeded in 96-well plates and grown for another 24 hours at 37°C in 0.1 mL medium, and then 10 μL methylthiazolotetrazolium solution, 5 mg/mL in phosphate-buffered saline (MTT; Sigma, St Louis, MO), was added and incubated for 3 hours, and the developed color was read at 570 nm. The cytotoxicity of H<sub>2</sub>O<sub>2</sub> was studied as described.<sup>24</sup> Briefly, at day 6 after transfections, 2 × 10<sup>4</sup> cells per well were seeded in 96-well plates, grown for 18 hours, and then washed and treated with different concentrations of H<sub>2</sub>O<sub>2</sub> for 2 hours in serum-free medium. The plates were washed twice, and cellular viability was measured after 3-hour incubation with MTT, as above under "HeLa cell transfection."

### Cellular incorporation of <sup>55</sup>Fe

HeLa cells at day 7 after transfections were incubated for 3 hours with 2 μCi/mL (0.074 MBq) (<sup>55</sup>Fe) ferric ammonium citrate (FAC) as previously described.<sup>25</sup> The cells were washed, lysed in 0.2 mL lysis buffer, and centrifuged, and 5 μL of the soluble fraction was mixed with 1 mL of ready safe liquid scintillation cocktail (Beckman, Hialeah, FL) and counted in a scintillation counter for 5 minutes. For the isolation of mitochondrial and postmitochondrial fractions, the cells were treated with 0.01% digitonin followed by 2 differential centrifugations, as described.<sup>26</sup> The soluble proteins were run on 7% nondenaturing polyacrylamide gel electrophoresis (PAGE), and the dried gels were exposed to autoradiography. The intensity of ferritin subunit bands was quantified by densitometry in the linear range.

### Biochemical and immunologic methods

L-ferritin levels were determined with a commercial serum ferritin assay, following the manufacturer's instructions (Abbott Laboratories, Abbott Park, IL). H-ferritin levels were evaluated by an enzyme-linked immunosorbent assay (ELISA) based on a specific monoclonal antibody and recombinant H-ferritin.<sup>27</sup> In immunoblot experiments, 30 μg soluble proteins was loaded on 12% SDS-PAGE. After transfer, the nitrocellulose filters were incubated for 16 hours with specific antibodies, washed, and further incubated for 1 hour with secondary peroxidase-labeled antibody (Dako, Glostrup, Denmark). Bound activity was revealed by advance enhanced chemiluminescence (ECL) kit (Amersham, Uppsala, Sweden) and detected using KODAK Image Station 440CF (Kodak, Rochester, NY). The primary antibodies used were mouse anti-TfR1 antibody (1:1000; Zymed, South San Francisco, CA), rabbit anti-poly(adenosine diphosphate-ribose) polymerase (anti-PARP) p85 fragment (1:700; Promega, Madison, WI), rabbit antiactin antibody (1:1000; Sigma), rabbit antiferritin antibody (1:2000; Sigma), mouse anti-MtF antibody, rabbit anti-MnSOD antibody (1:4000; Upstate, Billerica, MA), and rabbit antifibraxin antibodies (1:2000).<sup>28</sup>

For the determination of ATP levels, 1 × 10<sup>4</sup> cells were plated in 96-well culture black plates (Corning, Corning, NY) and lysated with the same volume of CellTiter-Glo Luminescent Cell Viability Assay (Promega), and the luminescence was analyzed. For the determination of the activity of aconitase, citrate synthase, succinate dehydrogenase, and superoxide dismutase, we followed previously described methods.<sup>29-32</sup> Cell apoptosis was measured by flow cytometry, using the ANNEXIN V:FITC assay kit (Serotec, Martinsried/Munich, Germany), following the manufacturer's instructions. Mitochondrial membrane potential ( $\Delta\Psi$ ) was measured using the red fluorescent dye JC-1 (Invitrogen-Molecular Probes, Eugene, OR). Protoporphyrin content was evaluated by flow cytometry as in Luksiene et al.<sup>33</sup>

### RNA extraction and real-time reverse-transcriptase-polymerase chain reaction (RT-PCR)

RNA was purified from cells using the guanidinium thiocyanate-phenol-chloroform method according to the manufacturer's instructions (RNAwiz;

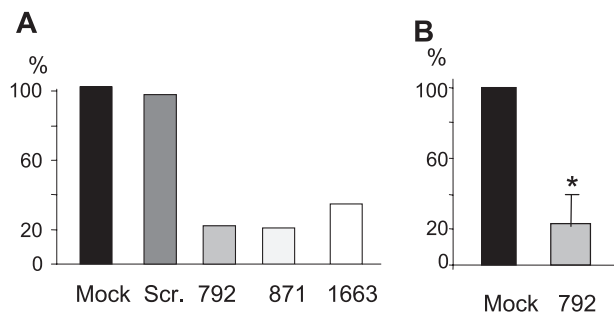


**Figure 1. Efficiency of ABCB7 siRNAs.** HeLa cells were transfected with 100 pmol of the indicated siRNAs, and the level of ABCB7 mRNA was quantified by real-time RT-PCR. The results are expressed as percentage of the control mock-transfected cells. (A) The siRNAs coded 792, 871, and 1663 were obtained by *in vitro* transcription and the HeLa cells analyzed 48 hours after transfection. (B) The siRNA 792 was produced by chemical synthesis and used in 2 rounds of transfection, and the cells were analyzed 48 hours after the second transfection. Mean and SD of 4 experiments. Scr indicates scrambled siRNA. \*Significant difference ( $P < .05$ ).

Ambion, Austin, TX). DNase-treated total RNA (1  $\mu$ g) was used to synthesize the first strand of cDNA with the ImProm-II Reverse Transcription System (Promega), using oligo dT. For real-time PCR analysis, Assays-on-Demand products (20 $\times$ ) and TaqMan Master Mix (2 $\times$ ) from Applied Biosystems (Foster City, CA) were used, according to the manufacturer's instructions, and the reactions were run on ABI PRISM 7700 Sequence Detection System (Applied Biosystems) in a final volume of 25  $\mu$ L for 40 cycles. We analyzed the expression levels of ABCB7 and frataxin, and we normalized the results to GAPDH levels in each sample.

#### Statistical analysis

Comparison of values between mock and transfected cells was performed by Student *t* test for unpaired data. Differences were defined as significant for *P* values less than .05.

## Results

### Production and analysis of siRNA for ABCB7

We initially produced by *in vitro* transcription 3 ds-siRNAs for ABCB7 silencing and set up the conditions for their transfection in HeLa cells. The siRNAs targeted mRNA sequences starting at nts 792, 871, and 1663. Real-time RT-PCR analysis of ABCB7 transcript showed that the highest level of inhibition was reached 48 hours after transfection, and that the 3 siRNAs used at the concentration of 100 pmol/well were efficient, leaving a residual level of transcript below 30% of the control and mock-transfected cells (Figure 1A). The most potent of them, named 792, was produced by chemical synthesis and its use optimized. At a concentration of 100 pmol/well, it caused up to 90% of inhibition of ABCB7, and by performing 2 sequential transfections the suppression could be maintained for up to 7 days (Figure 1B). These conditions, which imply transfection with siRNA-792 at day 1 and day 4 and cell harvesting at day 7, have been used in the following studies.

### Growth defects in ABCB7-silenced cells

The first evident effect of ABCB7 silencing was a reduction of cell growth. The cells transfected with any of the 3 siRNAs, after both the first and second round of transfection, reached confluence later than the matched mock-transfected cells (not shown). Trypan blue-positive cells accounted for 4% of the total cells both in the silenced and control cells, indicating the siRNAs did not cause cell death. Therefore, we analyzed the number of the viable cells that

excluded the dye, 3 days after the second round of transfection. In the silenced cells, this was about 50% of the mock-transfected control cells plated and grown under the same conditions (Figure 2A). When the same amounts of cells were seeded and grown for 24 hours, the MTT viability of the silenced cells was only approximately 60% of that of the controls (Figure 2B). Immunoblotting with specific antibodies did not show PARP fragmentation nor did flow cytometry show activation of annexin V (not shown), both of which are accepted signs of apoptosis. Moreover, we did not observe significant release of LDH, used as a sign of active necrotic processes (not shown). Thus, the reduction in cell viability in the silenced cells seemed to be caused by a reduction of cell proliferation rate, rather than by an increase of cell death.

### ABCB7 silencing and aconitase activity

Cytosolic aconitase/IRP1 is a Fe/S enzyme, and therefore it was of interest to evaluate if its activity was inhibited by ABCB7 silencing. In initial analysis, we measured aconitase activity in the total cellular extracts and in the postmitochondrial fraction to find that both of them were reduced in the silenced cells to about 50% and 40%, respectively (Figure 3A). For a more accurate analysis, the cellular extracts were separated in non-denaturing PAGE and the aconitase activity was developed.<sup>17</sup> The slower and more abundant band recovered in the mitochondrial fraction represented the mitochondrial aconitase (m-aco), while the faster band recovered in the postmitochondrial fraction consisted of the cytosolic aconitase (c-aco) (Figure 3B). ABCB7 silencing caused a reduction of approximately 50% of m-aco, and more than 80% of c-aco (Figure 3B) without a reduction of c-aco protein, determined by Western blotting (not shown). A similar effect was obtained by treating the cells for 18 hours with the iron chelator desferrioxamine (DFO, 1 mM), as already described.<sup>17</sup> We also treated the cells for 18 hours with carbonyl cyanide *m*-chloro phenyl hydrazone (CCCP, 30  $\mu$ M), under conditions to abolish mitochondrial membrane potential and inhibit iron uptake in the organelle.<sup>7</sup> This resulted in an inhibition of m-aco and of c-aco similar to that observed with ABCB7 silencing. When the silenced cells were treated with CCCP or with DFO, the activity of m-aco was further inhibited more than 80%, and that of c-aco became almost undetectable. The treatments with DFO and CCCP increased the proportion of unviable cells that detached from the plates (about 20% and 50%, respectively). We analyzed only the viable cells, which showed a protein pattern in SDS-PAGE indistinguishable from the one of the control, untreated cells (not shown). This finding suggests that ABCB7 deficiency inhibits the formation of Fe/S in c-aco by reducing the transit of iron through mitochondria.

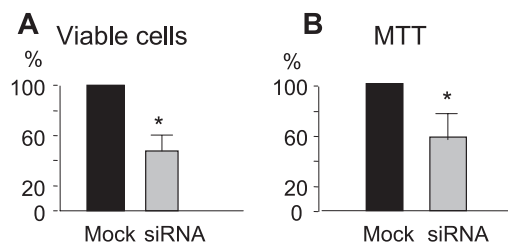


**Figure 2. Cell viability.** After the first round of mock or siRNA transfection, (A) 10<sup>5</sup> cells were seeded, transfected the following day, and grown for 3 days, and the viable cells that excluded trypan blue were counted. (B) Cell viability was also monitored by MTT assay after 24 hours of growth. The data are expressed as percentage of the control mock-transfected cells. Mean and SD of 10 experiments. The asterisks indicate a significant difference ( $P < .05$ ).

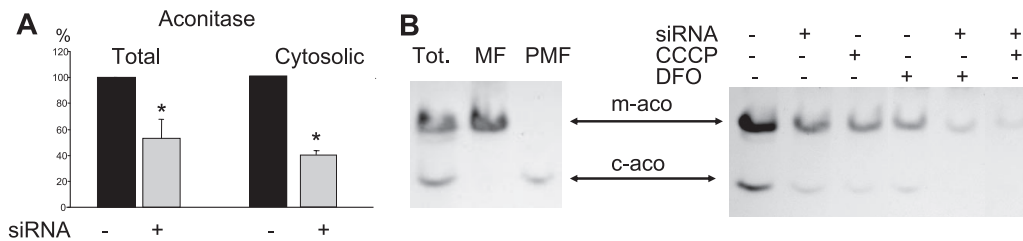
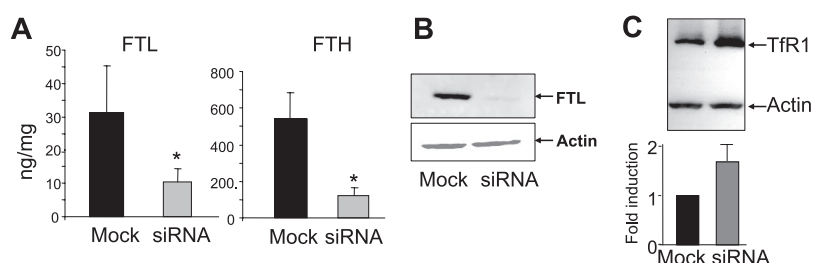


**Figure 3. Aconitase activity.** (A) The level of aconitase activity in the total cellular homogenates and in the postmitochondrial fraction was analyzed and expressed as percentage of the activity of the control mock-transfected cells. Mean and SD of 7 experiments for the total and of 3 experiments for the cytosolic aconitase. \*Significant difference ( $P < .05$ ). (B, left) The total cell homogenates of untreated HeLa cells (Tot), the mitochondrial fraction (MF), and the postmitochondrial fraction (PMF) were separated on nondenaturing PAGE, and the activity of aconitase was revealed. The fast band corresponds to the cytosolic aconitase (c-aco), while the slower band, to the mitochondrial isoform (m-aco). (Right) HeLa cells, transfected with ABCB7 siRNA (siRNA), treated for 18 hours with 30  $\mu$ M CCCP to abolish membrane potential, or for 18 hours with the iron chelator desferrioxamine 1 mM (DFO), as indicated, were analyzed for aconitase activity. Wells were loaded with 100  $\mu$ g proteins, and the load was verified by protein stain of the gel.

### Silencing of ABCB7 in HeLa cells affects cellular iron metabolism

The reduction of c-aco activity in the silenced cells was an index of cellular iron starvation. H- and L-ferritins are other reliable indices of iron status, and their levels, determined by ELISAs, were less than one third in the silenced cells compared with the controls (Figure 4A). The decrease in ferritin level was even more evident in immunoblotting with an antibody specific for L-ferritin (Figure 4B). Blotting showed also that the level of transferrin receptor 1 (TfR1) increased by 2-fold in the silenced cells (Figure 4C). Thus, all the indices showed that ABCB7 silencing caused an iron-deficient phenotype. To analyze more directly cellular iron homeostasis, the cells were incubated for 3 hours with radioactive ferric ammonium citrate,  $^{55}\text{Fe}$ -FAC, and then analyzed. The total iron incorporation in the silenced cells was about 20% lower than in the control cells, but the major difference was found in the subcellular distribution.  $^{55}\text{Fe}$  accumulated mostly in the cytosolic fraction of the control cells, while it was similarly distributed in the cytosolic and mitochondrial fraction in the ABCB7-silenced cells. For example, the ratio of  $^{55}\text{Fe}$  concentration in the postmitochondrial and mitochondrial fraction was higher than 7:1 in the controls and approximately 0.7:1 in the silenced cells (Figure 5A), indicating a major shift of iron from cytosol to mitochondria. Next, the homogenates were fractionated on nondenaturing PAGE and exposed to autoradiography. This showed a single band that corresponded to the cytosolic ferritin, the density of which was about 2-fold higher in the control than in the silenced cells, both in the total homogenate and in the postmitochondrial fraction (Figure 5B). The mitochondrial fractions displayed only a minor band corresponding to the cytosolic ferritin, probably a contaminant, while mitochondrial ferritin was undetectable (Figure 5B). Thus, ABCB7 silencing in HeLa cells caused a decrease of ferritin-bound iron in cytosol and a major increase of mitochondrial iron not firmly bound to any specific protein, without inducing the expression of mitochondrial ferritin (not shown).

**Figure 4. Indices of cellular iron status.** (A) After the double round of transfections, the content of H-ferritin (FTH) and L-ferritin (FTL) of the cell homogenates was evaluated by ELISA assays, and the data were expressed as nanogram of ferritin per milligram of total proteins. Mean and SD of 10 and of 3 different experiments for FTL and FTH, respectively; the asterisks indicate significant difference ( $P < .05$ ). (B) The ferritin content of the cell homogenates was evaluated by blotting from SDS-PAGE overlaid with anti-L-ferritin antibody. Actin was used for normalization. (C) Blotting of the cell homogenates with anti-transferrin receptor 1 (TfR1) antibodies. The level of expression relative to the control mock-transfected cells was quantified by gel densitometry in 3 different experiments and shown in the histogram. Data are shown as mean and SD of 3 experiments.



### Silencing of ABCB7 in HeLa cells increases sensitivity to $\text{H}_2\text{O}_2$

To verify if ABCB7 silencing and mitochondrial iron deposition affected the resistance to oxidative damage, the cells were incubated for 2 hours with various concentrations of  $\text{H}_2\text{O}_2$ , and then analyzed for cell viability with MTT assay. The 2 plots so obtained were statistically different ( $P = .009$ ), with that of the ABCB7-silenced cells being steeper than that of the mock-transfected control cells. The value of 50% inhibition was about 500  $\mu$ M for the controls and less than 200  $\mu$ M  $\text{H}_2\text{O}_2$  for the silenced cells (Figure 5C). Thus, ABCB7 deficiency causes a significant increase of sensitivity to  $\text{H}_2\text{O}_2$ .

### Mitochondrial enzymes, ATP, frataxin, and protoporphyrin

An increase in protoporphyrin IX is characteristic of XLSA/A, thus we evaluated if this occurred in the silenced cells. Protoporphyrin level was evaluated by flow cytometry taking advantage of the fluorescent properties of the molecule.<sup>33</sup> The basal level of fluorescence in the control cells was low, consistent with the low level of porphyrin synthesis in the HeLa cells, but it increased in the silenced cells. In 4 different experiments, we found a mean increase of the signal of 1.33-fold;  $P = .008$  (Figure 6D). The activity of succinate dehydrogenase, a mitochondrial Fe/S enzyme, was reduced by about 20% in the silenced cells, but the difference was not statistically significant. The activity of citrate synthase, a mitochondrial iron-free enzyme, was not affected by ABCB7 silencing (Figure 6A). Staining with JC-1 did not show evident modification of mitochondrial membrane potential (not shown), while total ATP content was higher ( $\sim 1.5$ -fold) in the silenced cells than the controls (Figure 6B). These data suggest that mitochondrial functionality was not impaired by ABCB7 deficiency. Since it has been reported that in yeast the suppression of Atm1 caused a down-regulation of frataxin, both at the mRNA and protein level,<sup>34</sup> we evaluated if the same occurred in our system. Quantitative real-time RT-PCR did not show significant

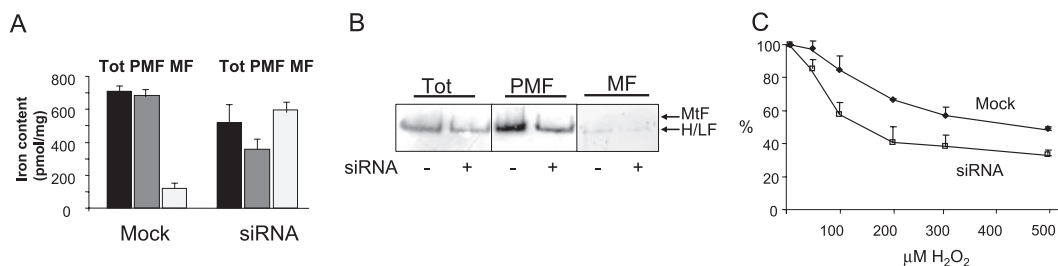


**Figure 5. Cellular iron incorporation and oxidative damage.** (A) Transfected and control cells were incubated for 3 hours with  $2 \mu\text{Ci/mL}$  ( $0.074 \text{ MBq}$ ) ( $^{55}\text{Fe}$ ) ferric ammonium citrate, and then the iron content was analyzed in the total cell extract (Tot), in the postmitochondrial fraction (PMF), and in the mitochondrial fraction (MF). The data are expressed as picomole  $^{55}\text{Fe}$  per milligram protein. Mean and SD of 4 experiments. (B) The 3 cellular fractions were loaded on nondenaturing PAGE ( $10 \mu\text{g}$  protein per lane), and then exposed to autoradiography to analyze protein-bound iron. A single band was evident, and it corresponded to the cytosolic H/L ferritin. The mobility of the mitochondrial ferritin (MtF) is indicated. (C) The mock-transfected controls and siRNA-transfected cells were incubated for 2 hours with various concentrations of  $\text{H}_2\text{O}_2$ , and then their viability was evaluated by MTT assay. Mean and SD of 3 experiments in octuplicate. The difference between the 2 plots was statistically highly significant ( $P = .009$ ).

modifications of the levels of frataxin and ferrochelatase mRNAs (data not shown). However, blotting with antifrataxin antibodies revealed that ABCB7 silencing caused a significant reduction of the mature form of the protein accompanied by a relative increase of the lighter degradation product (Figure 6C). This suggests a decrease of frataxin, probably due to faster degradation.

#### ABCB7 silencing in MtF-expressing cells

The expression of mitochondrial ferritin in HeLa cells was previously shown to cause a shift of iron from cytosol to mitochondria,<sup>25,35,36</sup> similar to that caused by ABCB7 silencing. Thus, it was of interest to compare the 2 cellular models. To this aim, we silenced ABCB7 in parallel in parent HeLa cells and in the HeLa clone expressing MtF (MtF clone). The cells were incubated for 3 hours with  $^{55}\text{Fe}$ , and the total iron incorporation in the 2 clones was not significantly different (not shown). The homogenates were fractionated, the iron content of mitochondrial and postmitochon-

drial fraction was analyzed, and the data were plotted as percentage of mitochondrial over the total cellular iron. This accounted for about 10% in the control HeLa cells, and it increased to 45% after ABCB7 silencing. Mitochondrial iron was about 40% in the MtF clone, and it was not affected by ABCB7 silencing (Figure 7A), possibly because the mechanism of mitochondrial iron incorporation was saturated. The silencing caused a reduction of iron bound to cytosolic ferritin (Figure 7B) and of H-ferritin protein (Figure 7B), similar to what has been observed in the HeLa cells (Figure 5B). Surprisingly, the band intensity of MtF-bound iron in the total cell homogenate and in the mitochondrial fraction was strongly reduced in the ABCB7-silenced cells (Figure 7B), without a significant decrease of MtF protein (Figure 7C). This indicates that the iron excess was not available to the ferritin. We analyzed superoxide dismutase activity in the cells, since it was shown that the activity of the mitochondrial Mn-SOD (SOD2) is affected by mitochondrial iron load in yeast.<sup>37</sup> The cytosolic SOD1 was not altered by ABCB7 silencing, while SOD2 was strongly inhibited in the parent HeLa cells but only marginally reduced in the MtF clone. Blotting with a specific antibody showed that SOD2 protein level was not affected, and thus ABCB7 silencing causes an inhibition of SOD2 activity (Figure 7D). Thus, as it occurs in yeast, the iron excess caused by ABCB7 silencing probably competes with Mn for binding to SOD2.

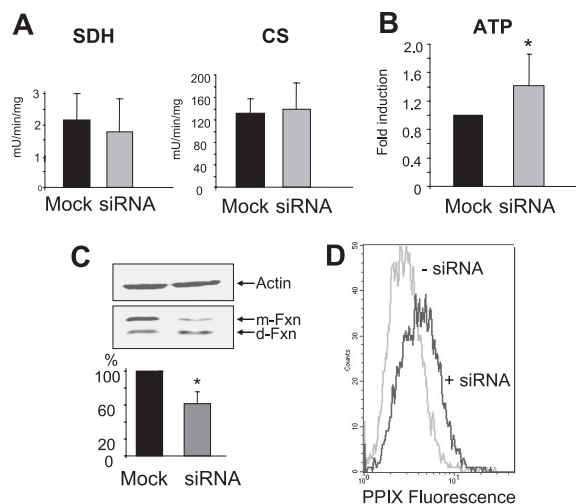


**Figure 6. Mitochondrial functionality.** (A) Activity of succinate dehydrogenase (SDH) and of citrate synthase (CS) in the cellular extracts of control and transfected cells. Mean and SD from 8 experiments, expressed as units per milligram total proteins. (B) Total ATP content of the cells expressed as fold increase over the control, mock-transfected cells; mean and SD of 6 experiments; the difference was statistically significant ( $*P = .038$ ). (C) Blotting analysis of frataxin expression in the control and transfected cells. Frataxin separates in a slower band corresponding to the mature form (m-Fxn) and a faster band corresponding to a degraded form (d-Fxn). In the silenced cells, the degraded form predominates. The relative content of total frataxin was evaluated by gel densitometry of 4 experiments as shown in the histogram. The difference was statistically significant ( $*P = .017$ ). (D) Histogram of protoporphyrin fluorescence of HeLa cells before ( $- \text{siRNA}$ ) and after ( $+ \text{siRNA}$ ) ABCB7 silencing. Data are representative of 4 independent experiments that showed an increase of 1.33-fold after silencing ( $P = .008$ ).

## Discussion

ABCB7 is a functional homolog of the yeast Atm1, a mitochondrial membrane protein involved in the maturation of cytosolic Fe/S proteins.<sup>20,38</sup> Mouse models showed that the absence of ABCB7 in most tissues, including CNS and bone marrow, is lethal, except for the liver and endothelial cells,<sup>22</sup> but did not clarify how its deficiency affected heme synthesis or produced neuronal defects. Thus, ABCB7's role in the development of sideroblastic anemia with ataxia (XLSA/A) remains obscure. We found conditions for an efficient inhibition of ABCB7 in HeLa cells by transfecting different specific siRNAs. All the siRNAs we developed were functional, inducing a decrease of the transcript level up to about 10% of the control. The silencing caused a large decrease in cellular proliferation, which hampered the possibility to obtain stable clones. For a better characterization of the phenotype, we extended the suppression of the protein up to 7 days by performing sequential siRNA transfections. A growth defect in cultured mammalian cells was already described for the depletion of the mitochondrial cysteine desulphurase m-Nfs1<sup>18,19</sup> and of frataxin,<sup>38</sup> and in yeast for the depletion of Atm1p<sup>39,40</sup> and of other proteins

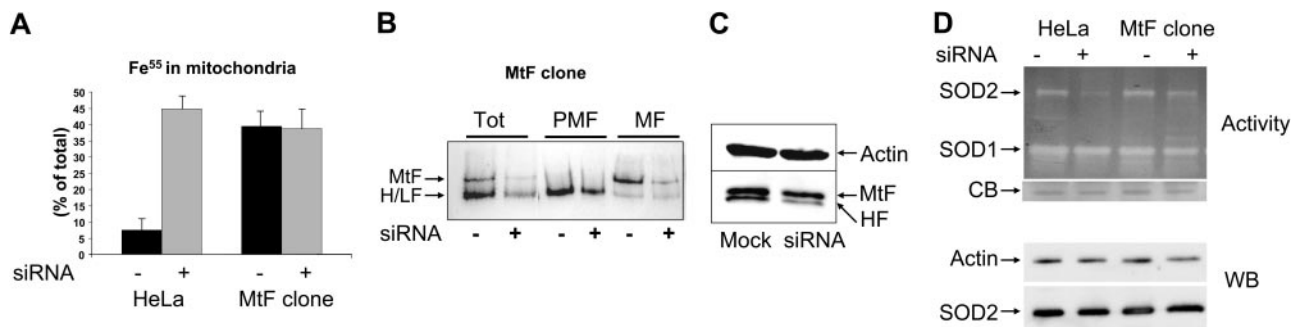


**Figure 7. ABCB7 silencing in MtF-expressing cells.** (A) The HeLa cell clone harboring a vector for the expression of MtF (MtF clone) was transfected with ABCB7-siRNA and then incubated with 2  $\mu$ Ci/mL (0.074 MBq) (<sup>55</sup>Fe) ferric ammonium citrate. After 3 hours, the cells were harvested and iron content was analyzed in the total and mitochondrial fractions. Iron incorporation in the mitochondria is expressed as percentage of total incorporated iron. In parallel are shown the data of MtF-free HeLa cells (HeLa) from Figure 5. Data are shown as mean and SD of 3 experiments. (B) The 3 cellular fractions were analyzed on nondenaturing PAGE and exposed to autoradiography to evaluate iron incorporation into cytosolic (H/L) and mitochondrial (MtF) ferritins. (C) Blotting with anti-MtF antibody of the total cellular extracts (30  $\mu$ g per lane) of control and transfected MtF clone, which recognizes MtF and H-ferritin (HF). Gel densitometry showed that MtF in the ABCB7-silenced cells is 80% of the control cells. (D) In the upper panel, the total cell homogenates (10  $\mu$ g) were analyzed for SOD activity by nondenaturing PAGE and nitroblue tetrazolium staining. SOD2 and SOD1 indicate activity of mitochondrial Mn SOD2 and of cytosolic SOD1 enzymes, respectively. CB indicates Coomassie blue stain of a band used for calibration of protein load. Lower panel shows SDS-PAGE Western blotting of the total homogenates (10  $\mu$ g) stained with anti-SOD2 (SOD2) and with antiactin antibody. Data are representative of 3 independent experiments with equivalent results.

involved in Fe/S biogenesis.<sup>7</sup> This was attributed to a defect in the maturation of cytosolic/nuclear Fe/S proteins involved in protein synthesis, such as Rli1p.<sup>8,9</sup> The growth defect caused by ABCB7 deficiency was not reversed by iron supplementation with 0.1 or 1 mM FAC, indicating that it was not due to iron deficiency, but possibly to the deregulation of the biosynthesis of cytosolic Fe/S proteins, and might contribute to the lethality of the model mice.

Another important effect of ABCB7 deficiency was a major accumulation of iron in the mitochondria, about 6-fold above control. This is similar to what has been found in the *Atm1p*-deficient yeast cells, where mitochondrial iron accumulation was up to 30-fold above control,<sup>7</sup> confirming that the 2 proteins are functional homologs involved in iron efflux from the organelle.<sup>39</sup> A mitochondrial iron deposition was not observed in the mouse livers in which ABCB7 was specifically inactivated,<sup>22</sup> a finding that was attributed to the unique control of iron metabolism in the liver or to a tissue-specific high expression of the ABCB6 mitochondrial transporter.<sup>22</sup> However, ABCB6 was recently shown to be a porphyrin transporter located on mitochondrial outer membrane,<sup>41</sup> and thus it should not contribute to Fe/S transport. Similarly to what occurs in yeast<sup>7</sup> and in mouse liver,<sup>22</sup> ABCB7 deficiency in HeLa cells did not cause major defects in mitochondrial activity, since SDH activity, membrane potential, and ATP content were not lower than those of the control cells. However, the massive iron loading of the mitochondria was expected to promote oxidative damage in HeLa cells. In fact, we could observe an increase of the sensitivity to H<sub>2</sub>O<sub>2</sub> toxicity, but the background levels of oxidation seemed normal. This is consistent with the low respiratory activity of these cultured mammalian cells, which consume little oxygen and have a small production of ROSs that would react with free iron to produce toxic-free radicals. Thus, the lack of evident oxidative damage in our cell model is not a demonstration that mitochondrial iron excess is harmless *in vivo*, particularly in cells with high iron needs and respiratory activity like those of the basal ganglia of the brain.<sup>42</sup> ABCB7 deficiency in HeLa cells and mouse liver caused major modification of cellular iron homeostasis, with activation of the IRE-BP activity of IRP1/c-aco and up-regulation of TfR1. In HeLa cells, this corresponded to an evident iron-deficient phenotype with a strong suppression of ferritin synthesis, partially attributed to the shift of iron from cytosol to mitochondria that could not be compensated by transferrin-iron uptake. In mouse hepatocytes, the cytosolic ferritin level was marginally increased, possibly due to the high iron influx due to constitutive activation of

TfR1 that has access to circulating Fe-transferrin, or to other compensatory mechanisms.<sup>22</sup>

In XLSA/A, microcytic anemia is accompanied by mitochondrial iron overload and accumulation of erythrocyte protoporphyrin, mostly as Zn-protoporphyrin.<sup>6,43-45</sup> Thus, defective heme synthesis occurs even in the presence of excess of the 2 components of heme molecule. Different hypotheses have been proposed. One is that ABCB7 binds ferrochelatase and increases its activity,<sup>21</sup> but this contrasts with the observation that most erythrocyte protoporphyrin in the patients is bound to Zn,<sup>43,44</sup> an association catalyzed by ferrochelatase,<sup>46</sup> and that ferrochelatase activity was not inhibited in the mouse model.<sup>22</sup> The second is that ABCB7 deficiency causes activation of IRP1, thus down-regulating the IRE containing ALAS2 and therefore heme synthesis.<sup>22</sup> This was found to occur in the Shiraz zebrafish model with glutaredoxin 5 deficiency, which also shows mitochondrial iron accumulation in erythroid cells, but this was accompanied by inhibition of protoporphyrin.<sup>47</sup> An activation of IRP1 seemed to occur in our silenced cells, but it did not inhibit protoporphyrin synthesis. A role of IRPs in heme synthesis is suggested by the finding that IRP2<sup>-/-</sup> mice accumulate erythrocyte protoporphyrin,<sup>48</sup> but this is probably as a result of local iron deficiency. A more likely explanation for the anemia is that the iron that accumulates in ABCB7 deficiency cannot be efficiently used for heme synthesis. This hypothesis is supported by the present finding that the iron excess in the ABCB7-silenced cells was poorly available to mitochondrial ferritin (MtF), in contrast with that of the mock-transfected control cells. This indicates that ABCB7 deficiency limits the pool of free Fe(II) ions available to MtF and to ferrochelatase, with a consequent increase of free protoporphyrin. The reduction of frataxin stability we observed may also be caused by an accumulation of apo-protein, possibly less stable than the Fe-bound form. The existence of biologically different mitochondrial iron pools has been recently demonstrated in yeast by the analysis of the mitochondrial Mn-SOD (SOD2).<sup>37</sup> One pool, termed SOD2-reactive, which competes with mitochondrial Mn to inactivate SOD2, increased in strains deleted of mitochondrial transporters and of proteins for Fe/S biosynthesis such as glutaredoxin-5 or *ssq1*, thus causing local iron accumulation. The other pool, termed SOD2-inert, did not affect SOD2 activity and was prominent in wild-type and frataxin-deficient cells.<sup>37</sup> We found that mitochondrial iron overload in the ABCB7-silenced cells inhibited SOD2 activity, indicating that a SOD2-reactive pool exists also in

mammalian cells. Our findings raise the possibility that the SOD2-reactive pool is made of iron committed for Fe/S synthesis and therefore is not available to ferritin or ferrochelatase, a hypothesis that needs to be proved.

Mitochondrial iron accumulation is particularly evident in erythroid cells, where most of body iron transits for hemoglobin synthesis. The formation of ringed sideroblasts (or siderocytes in mice) is probably caused by various different mechanisms. In the most common, acquired forms of sideroblastic anemia (SA), the refractory anemia with ringed sideroblasts (RARS), the sideroblasts express high levels of MtF.<sup>49-51</sup> Since this was found also in XLSA with defects of ALAS2,<sup>49</sup> it was initially thought that MtF expression was common to the different forms of SA. Our data indicate that MtF expression is not simply induced by mitochondrial iron accumulation, and in cultivated bone marrow erythroid cells from patients with RARS the expression of MtF was found to occur at early stages of differentiation before evident iron deposition.<sup>50,51</sup> Thus, in these forms of SA, MtF may contribute to mitochondrial iron deposition while protecting the organelle from the iron excess. In a mouse model of XLSA, the erythroid expression of MtF mRNA was not observed,<sup>52</sup> thus other mechanisms besides MtF expression contribute to this form of mitochondrial iron accumulation. Very little is known about the other genetic forms of SA, all of which seem to affect proteins with mitochondrial localization. They include mitochondrial DNA deletions in Pearson syndrome,<sup>53</sup> defects of pseudouridine synthase 1 (PUS1) in mitochondrial myopathy and sideroblastic anemia,<sup>54</sup> and defects of the mitochondrial transporters sideroflexin 1 in flexed tail mice,<sup>55</sup> while for the defects of SOD2 in mice, the anemia and mitochondrial iron deposition was attributed to oxidative damage.<sup>56</sup> XLSA/A is characterized by an excess of erythrocyte protoporphyrin, at

variance with all the other types of genetic SA, and we propose it is caused by the accumulation of an iron form not readily usable for heme synthesis. Possibly, this may contribute to other forms of SA, such as RARS, that also often show excess of erythrocyte protoporphyrin.<sup>57</sup> ABCB7 is ubiquitous, and its deficiency may cause mitochondrial iron deposition and sensitivity to oxidative damage in most cells, but the ones most sensitive seem to be those of the basal ganglia<sup>42</sup> whose degeneration may cause ataxia and movement disorders, similar to what occurs in Friedreich ataxia<sup>4</sup> and Pank2 disease.<sup>58</sup>

## Acknowledgments

The work was partially supported by a grant of Consorzio Interuniversitario per le Biotecnologie and by a Must-Cofin-2004 grant (P.A.).

We are grateful to Dr Wing-Hang Tong for the help in the development of aconitase gel assay. The antibody against human frataxin was a generous gift from Dr Franco Taroni.

## Authorship

Contribution: All authors participated in designing and performing the research. P.C and P.A. wrote the paper, and all authors checked the final version of the paper.

Conflict-of-interest disclosure: The authors declare no competing financial interests.

Correspondence: Paolo Arosio, Dipartimento Materno Infantile e Tecnologie Biomediche, Università di Brescia, Viale Europa 11, 25123 Brescia, Italy; e-mail: arosio@med.unibs.it.

## References

- Hentze MW, Muckenthaler MU, Andrews NC. Balancing acts: molecular control of mammalian iron metabolism. *Cell*. 2004;117:285-297.
- Lill R, Muhlenhoff U. Iron-sulfur-protein biogenesis in eukaryotes. *Trends Biochem Sci*. 2005;30:133-141.
- Napier I, Ponka P, Richardson DR. Iron trafficking in the mitochondrion: novel pathways revealed by disease. *Blood*. 2005;105:1867-1874.
- Pandolfo M. Friedreich ataxia. *Semin Pediatr Neurol*. 2003;10:163-172.
- Fleming MD. The genetics of inherited sideroblastic anemias. *Semin Hematol*. 2002;39:270-281.
- Allikmets R, Raskind WH, Hutchinson A, Schueck ND, Dean M, Koeller DM. Mutation of a putative mitochondrial iron transporter gene (ABC7) in X-linked sideroblastic anemia and ataxia (XLSA/A). *Hum Mol Genet*. 1999;8:743-749.
- Kispal G, Csere P, Prohl C, Lill R. The mitochondrial proteins Atm1p and Nfs1p are essential for biogenesis of cytosolic Fe/S proteins. *EMBO J*. 1999;18:3981-3989.
- Kispal G, Sipos K, Lange H, et al. Biogenesis of cytosolic ribosomes requires the essential iron-sulphur protein Rli1p and mitochondria. *EMBO J*. 2005;24:589-598.
- Yarunin A, Panse VG, Petfalski E, Dez C, Tollervy D, Hurt EC. Functional link between ribosome formation and biogenesis of iron-sulfur proteins. *EMBO J*. 2005;24:580-588.
- Hausmann A, Aguilar Netz DJ, Balk J, Pierik AJ, Muhlenhoff U, Lill R. The eukaryotic P loop NTPase Nbp35: an essential component of the cytosolic and nuclear iron-sulfur protein assembly machinery. *Proc Natl Acad Sci U S A*. 2005;102:3266-3271.
- Rutherford JC, Ojeda L, Balk J, Muhlenhoff U, Lill R, Winge DR. Activation of the iron regulon by the yeast Aft1/Aft2 transcription factors depends on mitochondrial but not cytosolic iron-sulfur protein biogenesis. *J Biol Chem*. 2005;280:10135-10140.
- Chen OS, Crisp RJ, Valachovic M, Bard M, Winge DR, Kaplan J. Transcription of the yeast iron regulon does not respond directly to iron but rather to iron-sulfur cluster biosynthesis. *J Biol Chem*. 2004;279:29513-29518.
- Lill R, Kispal G. Maturation of cellular Fe-S proteins: an essential function of mitochondria. *Trends Biochem Sci*. 2000;25:352-356.
- Gakh O, Park S, Liu G, et al. Mitochondrial iron detoxification is a primary function of frataxin that limits oxidative damage and preserves cell longevity. *Hum Mol Genet*. 2006;15:467-479.
- Li K, Tong WH, Hughes RM, Rouault TA. Roles of the mammalian cytosolic cysteine desulfurase, ISCS, and scaffold protein, ISCU, in iron-sulfur cluster assembly. *J Biol Chem*. 2006;281:12344-12351.
- Tong WH, Rouault T. Distinct iron-sulfur cluster assembly complexes exist in the cytosol and mitochondria of human cells. *EMBO J*. 2000;19:5692-5700.
- Tong WH, Rouault TA. Functions of mitochondrial ISCU and cytosolic ISCU in mammalian iron-sulfur cluster biogenesis and iron homeostasis. *Cell Metab*. 2006;3:199-210.
- Biederbick A, Stehling O, Rosser R, et al. Role of human mitochondrial Nfs1 in cytosolic iron-sulfur protein biogenesis and iron regulation. *Mol Cell Biol*. 2006;26:5675-5687.
- Fosset C, Chauveau MJ, Guillon B, Canal F, Drapier JC, Bouton C. RNA silencing of mitochondrial m-Nfs1 reduces Fe-S enzyme activity both in mitochondria and cytosol of mammalian cells. *J Biol Chem*. 2006;281:25398-25406.
- Csere P, Lill R, Kispal G. Identification of a human mitochondrial ABC transporter, the functional orthologue of yeast Atm1p. *FEBS Lett*. 1998;441:266-270.
- Taketani S, Kakimoto K, Ueta H, Masaki R, Furukawa T. Involvement of ABC7 in the biosynthesis of heme in erythroid cells: interaction of ABC7 with ferrochelatase. *Blood*. 2003;101:3274-3280.
- Pondarre C, Antiochos BB, Campagna DR, et al. The mitochondrial ATP-binding cassette transporter Abcb7 is essential in mice and participates in cytosolic iron-sulfur cluster biogenesis. *Hum Mol Genet*. 2006;15:953-964.
- Donze O, Picard D. RNA interference in mammalian cells using siRNAs synthesized with T7 RNA polymerase. *Nucleic Acids Res*. 2002;30:e46.
- Cozzi A, Corsi B, Levi S, Santambrogio P, Biasotto G, Arosio P. Analysis of the biologic functions of H- and L-ferritins in HeLa cells by transfection with siRNAs and cDNAs: evidence for a proliferative role of L-ferritin. *Blood*. 2004;103:2377-2383.
- Corsi B, Cozzi A, Arosio P, et al. Human mitochondrial ferritin expressed in HeLa cells incorporates iron and affects cellular iron metabolism. *J Biol Chem*. 2002;277:22430-22437.
- Tiranti V, Corona P, Greco M, et al. A novel frameshift mutation of the mtDNA COIII gene leads to impaired assembly of cytochrome c oxidase in a patient affected by Leigh-like syndrome. *Hum Mol Genet*. 2000;9:2733-2742.
- Cozzi A, Levi S, Bazzigaluppi E, Ruggeri G, Arosio P. Development of an immunoassay for all

- human isoferritins, and its application to serum ferritin evaluation. *Clin Chim Acta*. 1989;184:197-206.
28. Branda SS, Cavadini P, Adamec J, Kalousek F, Taroni F, Isaya G. Yeast and human frataxin are processed to mature form in two sequential steps by the mitochondrial processing peptidase. *J Biol Chem*. 1999;274:2763-2769.
  29. Gardner PR, Nguyen DD, White CW. Aconitase is a sensitive and critical target of oxygen poisoning in cultured mammalian cells and in rat lungs. *Proc Natl Acad Sci U S A*. 1994;91:12248-12252.
  30. Williamson JR, Corkey BE. Assay of citric acid cycle intermediates and related compounds-update with tissue metabolite levels and intracellular distribution. *Methods Enzymol*. 1979;55:200-222.
  31. Munujos P, Coll-Canti J, Gonzalez-Sastre F, Gella FJ. Assay of succinate dehydrogenase activity by a colorimetric-continuous method using iodinitro-tetrazolium chloride as electron acceptor. *Anal Biochem*. 1993;212:506-509.
  32. White CW, Nguyen DH, Suzuki K, et al. Expression of manganese superoxide dismutase is not altered in transgenic mice with elevated level of copper-zinc superoxide dismutase. *Free Radic Biol Med*. 1993;5:629-636.
  33. Luksiene Z, Eggen I, Moan J, Nesland JM, Peng Q. Evaluation of protoporphyrin IX production, phototoxicity and cell death pathway induced by hexylester of 5-aminolevulinic acid in Reh and HPB-ALL cells. *Cancer Lett*. 2001;169:33-39.
  34. Schueck ND, Wootner M, Koeller DM. The role of the mitochondrion in cellular iron homeostasis. *Mitochondrion*. 2001;1:51-60.
  35. Levi S, Corsi B, Bosisio M, et al. A human mitochondrial ferritin encoded by an intronless gene. *J Biol Chem*. 2001;276:24437-24440.
  36. Nie G, Sheftel AD, Kim SF, Ponka P. Overexpression of mitochondrial ferritin causes cytosolic iron depletion and changes cellular iron homeostasis. *Blood*. 2005;105:2161-2167.
  37. Yang M, Cobine PA, Molik S, et al. The effects of mitochondrial iron homeostasis on cofactor specificity of superoxide dismutase 2. *EMBO J*. 2006;25:1775-1783.
  38. Bekri S, Kispal G, Lange H, et al. Human ABC7 transporter: gene structure and mutation causing X-linked sideroblastic anemia with ataxia with disruption of cytosolic iron-sulfur protein maturation. *Blood*. 2000;96:3256-3264.
  39. Stehling O, Elsasser HP, Bruckel B, Muhlenhoff U, Lill R. Iron-sulfur protein maturation in human cells: evidence for a function of frataxin. *Hum Mol Genet*. 2004;13:3007-3015.
  40. Leighton J, Schatz G. An ABC transporter in the mitochondrial inner membrane is required for normal growth of yeast. *EMBO J*. 1995;14:188-195.
  41. Krishnamurthy PC, Du G, Fukuda Y, et al. Identification of a mammalian mitochondrial porphyrin transporter. *Nature*. 2006;443:586-589.
  42. Zecca L, Youdim MB, Riederer P, Connor JR, Crichton RR. Iron, brain ageing and neurodegenerative disorders. *Nat Rev Neurosci*. 2004;5:863-873.
  43. Pagon RA, Bird TD, Detter JC, Pierce I. Hereditary sideroblastic anaemia and ataxia: an X linked recessive disorder. *J Med Genet*. 1985;22:267-273.
  44. Hellier KD, Hatchwell E, Duncombe AS, Kew J, Hammans SR. X-linked sideroblastic anaemia with ataxia: another mitochondrial disease? *J Neurol Neurosurg Psychiatry*. 2001;70:65-69.
  45. Maguire A, Hellier K, Hammans S, May A. X-linked cerebellar ataxia and sideroblastic anaemia associated with a missense mutation in the ABC7 gene predicting V411L. *Br J Haematol*. 2001;115:910-917.
  46. Jacobs JM, Sinclair PR, Sinclair JF, et al. Formation of zinc protoporphyrin in cultured hepatocytes: effects of ferrochelatase inhibition, iron chelation or lead. *Toxicology*. 1998;125:95-105.
  47. Wingert RA, Galloway JL, Barut B, et al. Deficiency of glutaredoxin 5 reveals Fe-S clusters are required for vertebrate haem synthesis. *Nature*. 2005;436:1035-1039.
  48. Cooperman SS, Meyron-Holtz EG, Olivierre-Wilson H, Ghosh MC, McConnell JP, Rouault TA. Microcytic anemia, erythropoietic protoporphyria, and neurodegeneration in mice with targeted deletion of iron-regulatory protein 2. *Blood*. 2005;106:1084-1091.
  49. Cazzola M, Invernizzi R, Bergamaschi G, et al. Mitochondrial ferritin expression in erythroid cells from patients with sideroblastic anemia. *Blood*. 2003;101:1996-2000.
  50. Tehrani R, Invernizzi R, Grandine A, et al. Aberrant mitochondrial iron distribution and maturation arrest characterize early erythroid precursors in low-risk myelodysplastic syndromes. *Blood*. 2005;106:247-253.
  51. Della Porta MG, Malcovati L, Invernizzi R, et al. Flow cytometry evaluation of erythroid dysplasia in patients with myelodysplastic syndrome. *Leukemia*. 2006;20:549-555.
  52. Nakajima O, Okano S, Harada H, et al. Transgenic rescue of erythroid 5-aminolevulinic acid synthase-deficient mice results in the formation of ring sideroblasts and siderocytes. *Genes Cells*. 2006;11:685-700.
  53. Casademont J, Barrientos A, Cardellach F, et al. Multiple deletions of mtDNA in two brothers with sideroblastic anemia and mitochondrial myopathy and in their asymptomatic mother. *Hum Mol Genet*. 1994;3:1945-1949.
  54. Casas KA, Fischel-Ghodsian N. Mitochondrial myopathy and sideroblastic anemia. *Am J Med Genet A*. 2004;125:201-204.
  55. Fleming MD, Campagna DR, Haslett JN, Trenor CC III, Andrews NC. A mutation in a mitochondrial transmembrane protein is responsible for the pleiotropic hematological and skeletal phenotype of flexed-tail (*ft/ft*) mice. *Genes Dev*. 2001;15:652-657.
  56. Friedman JS, Lopez MF, Fleming MD, et al. SOD2-deficiency anemia: protein oxidation and altered protein expression reveal targets of damage, stress response, and antioxidant responsiveness. *Blood*. 2004;104:2565-2573.
  57. Steensma DP, Hecksel KA, Porcher JC, Lasho TL. Candidate gene mutation analysis in idiopathic acquired sideroblastic anemia (refractory anemia with ringed sideroblasts). *Leuk Res*. Prepublished on July 24, 2006, as DOI 10.1016/j.leukres.2006.06.005.
  58. Hayflick SJ. Unraveling the Hallervorden-Spatz syndrome: pantothenate kinase-associated neurodegeneration is the name. *Curr Opin Pediatr*. 2003;15:572-577.